# VLBI OBSERVATIONS OF SOUTHERN EGRET IDENTIFICATIONS. II. VLBA OBSERVATIONS AND THE IMPORTANCE OF JET BENDING IN GAMMA-RAY SOURCES

S.J. Tingay and D.W. Murphy

Jet Propulsion Laboratory, California Institute of Technology (MS238-332), 4800 Oak Grove Drive, Pasadena, CA 91109

email: tingay@hyaa.jpl.nasa.gov, dwm@casa.jpl.nasa.gov

P.G. Edwards

Institute of Space and Astronautical Science, Sagamihara, Kanagawa 229, Japan

email: pge@vsop.isas.ac.jp

Received _____; accepted _____

## ABSTRACT

We present VLBI images of 6 Southern Hemisphere radio sources which have been identified by EGRET as sources of greater than 100 MeV gamma-ray emission, PKS 0521−365, PKS 1127−145, PKS 1622−253, PKS 1627−297, PKS 1730−130, and PKS 1908−201, completing the observation of all EGRET-identified sources south of $\delta = -10°$. We quantitatively investigate the suggestion of von Montigny et al. (1995) that jet bending may be a significant factor affecting the gamma-ray identification of radio loud, flat-spectrum AGN, using samples of EGRET-identified and gamma-ray quiet radio sources. From this investigation we find evidence to suggest that jet bending properties, as observed in pc-scale radio jets, are correlated with gamma-ray identification for this class of source. The pc-scale jets in gamma-ray quiet AGN appear to have more and larger bends than the pc-scale jets in EGRET-identified AGN. Caution should be exercised when interpreting these results however, since we point out that significant, but difficult to quantify, observational biases may also be at work in these samples.

*Subject headings:* galaxies:active–galaxies:jets–gamma rays:observations – techniques:interferometric

## 1. INTRODUCTION

The identification of over 40 active galactic nuclei (AGN) as sources of greater than 100 MeV gamma-ray emission by the EGRET instrument aboard the *Compton Gamma-Ray Observatory* (Thompson et al. 1995; Mattox et al. 1997b; Punsley 1997) has opened up a wavelength range previously out of reach for the investigation of active galaxies, prompting both observational (e.g. Fichtel et al. 1994; Thompson et al. 1995; von Montigny et al. 1995; Moellenbrock et al. 1996; Tingay et al. 1996; Impey 1996; Mattox et al. 1997b; Comastri et al. 1997) and theoretical (e.g. Salamon and Stecker 1994; Dondi and Ghisellini 1995; Romanova and Lovelace 1997; references in Fichtel et al. 1994) studies of the properties of gamma-ray loud AGN. One of the most significant observational results of these studies to date is that all of the extragalactic gamma-ray sources thus far identified have been associated with strong, flat-spectrum radio sources, in particular compact core-jet radio sources such as core dominated quasars and BL Lac type objects.

Based on this result it has been postulated that the gamma-ray emission from extragalactic sources, favored as inverse Compton emission, originates deep within the relativistic jet of the AGN and is beamed toward us. This postulate appears to qualitatively fit the general properties of the EGRET-identified AGN: the very high, up to $3\times10^{49}$ ergs $s^{-1}$ (Mattox et al. 1997a) gamma-ray luminosities; the core dominated nature of the associated radio sources; the high incidence of apparent superluminal motions; and the high incidence of rapid variability at all wavelengths.

It has also been suggested that relativistic beaming may explain the observation that although all EGRET-identified AGN are radio loud with flat spectra, not all radio loud, flat-spectrum AGN are detectable gamma-ray sources. One way in which this can happen is if the region of an AGN jet where the gamma-ray emission originates produces a narrower beaming cone than the radio emitting region, for example by virtue of a higher jet speed

in the gamma-ray emitting region than in the radio emitting region. In this case the gamma-ray emission could be beamed away from our line of sight, or Doppler dimmed, while the radio emission could still be Doppler boosted by virtue of a wider beaming cone (Salamon & Stecker 1994). A second possibility could involve a jet which bends downstream of the gamma-ray emitting region before the radio emission is produced. In this case, again, the gamma-ray emission could be beamed away from our line of sight but the radio emission could still be beamed towards us by virtue of the better alignment of the jet at this point with our line of sight (von Montigny et al. 1995).

In principle it is possible to investigate the importance of relativistic beaming for gamma-ray production in EGRET-identified AGN. One can determine if beaming is a significant factor affecting the probability of AGN identification in gamma-rays by observing well defined samples of EGRET-identified and gamma-ray quiet radio sources and making a comparison of the two samples, based on parameters which are indicators of relativistic beaming, e.g. apparent jet speed (pc-scale), core dominance (kpc-scale), radio core brightness temperature (pc-scale). In particular, VLBI observations which allow us to image the emission from an AGN directly, as close as is possible to the region of the jet where the gamma-ray emission is suggested to occur, may give the best estimates for the degree of relativistic beaming of the gamma-ray emission.

Previously, using 22 GHz transcontinental VLBI observations, Moellenbrock et al. (1996) noted that of 140 bright radio sources, EGRET-identified radio sources had an average radio core brightness temperature and correlated flux density significantly higher than the gamma-ray quiet sources in the sample. Mattox et al. (1997b) found a similar result from the older 2.29 GHz VLBI flux densities of Preston et al. (1985), where the EGRET-identified radio sources were brighter, on average, than the gamma-ray quiet radio sources. Similarly Zhou et al (1997) claims a correlation between gamma-ray and VLBI

radio luminosities for the EGRET-identified radio sources. Impey (1996) found a significant difference between EGRET-identified and gamma-ray quiet radio sources in total 5 GHz flux density, with EGRET-identified sources being, on average, brighter than gamma-ray quiet radio sources. These results are consistent with relativistically beamed radio emission being correlated with the identification of AGN in gamma-rays. On the other hand, Impey (1996) found no significant difference in radio core dominance between EGRET-identified and gamma-ray quiet radio sources and Tingay et al. (1996; hereafter Paper I) investigated the superluminal motion statistics from the literature for EGRET-identified and gamma-ray quiet core dominated radio sources and found no significant difference.

We feel that more work needs to be done to conclusively demonstrate, or rule out, that relativistic beaming is the dominant factor which affects the apparent gamma-ray strength of an AGN, although it seems likely that it is at least a partial factor, given the results of previous investigations. With this as our motivation, in this paper we continue with our work of Paper I, presenting new VLBI imaging results for 6 Southern Hemisphere EGRET-identified radio sources in §3 which, together with the results from Paper I, and the investigations of other authors, completes the VLBI observation of all EGRET-identified radio sources south of $\delta = -10°$.

We continue to investigate possible differences between the EGRET-identified radio sources and similar gamma-ray quiet radio sources, in light of the relativistic beaming paradigm. In §4 we discuss the interesting possibility, put forward by von Montigny et al. (1995), that bent or misaligned jets are preferentially associated with gamma-ray quiet radio sources and that straight, aligned jets are associated with EGRET-identified radio sources, using observational data from §3 and collected from the literature.

## 2. OBSERVATIONS AND DATA REDUCTIONS

Observations of 5 EGRET-identified AGN between the declinations of $-10°$ and $-40°$ were obtained with the full VLBA on 1997 Feb. 17 over a 20 hr period at 8.387 GHz. For two sources, PKS 0521−365 and PKS 1127−145, continuous tracks in the $u - v$ plane were obtained for approximately 6 and 4 hr, respectively. In the remaining 10 hr of the experiment the array switched between the remaining three sources, PKS 1622−253, PKS 1730−130, and PKS 1908−201, obtaining broken tracks with ten minutes of data on each source every half an hour. Single polarization recording was used with 1 bit sampling and a 64 MHz bandwidth split into 8 IF's, each consisting of sixteen 0.5 MHz channels. The VLBA data were calibrated and fringe-fit using the standard routines in the recomended reduction path for VLBA data described in the AIPS cookbook. The amplitude calibrated and fringe-fit data were exported from AIPS as FITS files and read into the DIFMAP difference mapping software (Shepherd, Pearson, and Taylor, 1994) for imaging.

Images were produced using mapsizes of 512 pixels and pixel sizes ranging between 0.1 and 0.3 mas. Phase-only self-calibration was performed initially using a point source model to straighten the phases, following which the data were coherently averaged in time onto a 30 second grid and edited. Tight clean windows were used initially on the core and then for any extended structure. Phase self-calibration was used until the total flux density of the model components accounted for the flux density of the shorter baselines of the array and then amplitude self-calibration was performed over a time-scale much longer than the duration of the observation. Subsequent amplitude self-calibration steps used shorter and shorter time-scales, until point-to-point amplitude self-calibration was performed and the image completed.

In addition to our new VLBA observations, we have obtained data from the VLBA public archives for PKS 1622−297, observed at 1.651 and 4.979 GHz on 1994 Sep. 1 and

1994 August 8, respectively (1 bit sampling, 16 MHz bandwidth). These data consisted of 2 ten minute scans separated by approximately 2 hr, producing a $u - v$ coverage usable for imaging. The data were reduced as per the general procedure given above for the 1997 Feb. 17 VLBA observations. One difference in the reduction technique was that for the PKS 1622−297 data, before fringe-fitting, a manual calibration of the instrumental delays and channel phase offsets was required.

Radio core brightness temperatures were determined from the images for all 6 sources, following the description given in Paper I.

## 3. THE INDIVIDUAL SOURCES

### 3.1. PKS 0521−365

PKS 0521−365 is the second closest of the EGRET-identified AGN (Thompson et al. 1995; Lin et al. 1995) at a red shift of z=0.055 and has previously been investigated by us with VLBI at 4.8 and 8.4 GHz. VLBI images from 1992 and 1993 have shown this source to have a compact core with brightness temperature $1.1\times10^{11}$ K (core size 0.8 × 0.6 mas and flux density 1.2 Jy at 4.8 GHz) and a jet extending approximately 10 mas from the core along position angle 310°±5° (Paper I). The total flux density of the source has remained stable over the past 12 months (Tingay et al. in preparation).

Figure 1 shows the new VLBA image of PKS 0521−365. The bright core component is evident at the south-east end of the source and the jet extends along a position angle of 312°, aligning well with the kpc-scale structure as found in Paper I. However, it is apparent that a significant change in the source structure has taken place over the last three years. The brightest component in the jet now lies approximately 27 mas from the core, compared to $10.3^{+1.2}_{-1.8}$ on 1993 Oct. 21, at the same observing frequency (Paper I). Two fainter

components lie between the core and the 27 mas component in Figure 1. A re-analysis of data from Paper I, intended to enhance the detectability of structure as extended as seen in Figure 1, failed to show any emission more extended than seen in the images presented in Paper I.

We have model-fit the new VLBA $u - v$ data for PKS 0521−365 to quantify the structure seen in Figure 1. Table 2 contains the model-fitting results. In comparison, the model-fitting of the 8.4 GHz observations of 1993 October 21 (Paper I) is in terms of only two components, the core (which is clearly extended in the direction of the jet) and the 10.3 mas component. We tentatively suggest that the 10.3 mas component on 1993 October 21 is the 27 mas component seen in the new VLBA image, and that the component seen in Figure 1 and described in Table 2 near 19 mas may correspond to the core extension at 1993 October 21 - at both epochs the separation between these two components is approximately 8 mas.

If this interpretation is correct then these two components have moved approximately 16.7 mas in 3.3 yr, relative to the core, corresponding to 5.1 mas $\mathrm{yr}^{-1}$ or $13.6\mathrm{h}^{-1}\mathrm{c}$ at the red shift of PKS 0521−365 (assuming $q_0 = 0$ and $H_0 = 100h$). At this rate, the component seen in Figure 1 approximately 11 mas from the core would have been ejected early in 1995. This estimate for the superluminal motion of PKS 0521−365 is not unreasonable when compared to estimates for other compact radio sources (Vermuelen & Cohen 1994) and is consistent with the model-fitting of PKS 0521−365 from Paper I. However, confirmation needs to come with at least one further epoch of VLBA observation and images similar in resolution to Figure 1.

The radio core brightness temperature of PKS 0521−365 at 8.387 GHz was found to be approximately $5\times10^{10}$ K (core flux density of 1.7 Jy and core dimensions of 1.3 × 0.5 mas), half of what was estimated at 4.8 GHz in Paper I.

### 3.2. PKS 1127−145

PKS 1127−145 is a well known low frequency variable radio source (Wehrle et al. 1992; Bondi et al. 1996) at a redshift of z=1.187 which was identified in the second EGRET catalog (Thompson et al. 1995). Bondi et al. (1996) presents VLBI data from three epochs of observation at 18 cm, spanning 1980.1 to 1987.9, which show no significant structural variations. Wehrle et al. (1992) presents a VLBI image at 4.991 GHz from 1988 August 6 which shows that the jet emerges from the core at a position angle of 81° and bends through −29° approximately 3 mas from the core. The final direction of the pc-scale jet (52°) aligns reasonably well with the position angle of the extended radio structure on the kpc-scale. Flux density monitoring from the Australia Telescope Compact Array (ATCA) shows small variations in the cm wavelength radio emission and an inverted spectral index between 2.3 and 8.6 GHz (Tingay et al. in preparation).

Figure 2 shows the image from our new VLBA data for PKS 1127−145 at 8.387 GHz. This image agrees well with the image of Wehrle et al. (1992). The core is evident at the western end of the source. Approximately 4 mas from the core a bright component dominates the jet, following which the jet bends through 30°.

The radio core brightness temperature of PKS 1127−145 at 8.387 GHz was found to be approximately $2\times10^{11}$ K (core flux density of 1.4 Jy and core dimensions of 0.6 × 0.2 mas).

### 3.3. PKS 1622−253

PKS 1622−253 is a highly variable radio source identified as an gamma-ray source in the second EGRET catalog. EGRET observations between April 1991 and September 1993 yield a value of 2.27±0.24 for the gamma ray spectral index (Nolan et al. 1996). The 5 GHz flux given in the Parkes90 catalog is 2.02 Jy, however in the PMN survey (Griffith et al.

1994) a flux at 4.85 GHz of 3.5 Jy is reported. Recent flux density monitoring observations at the ATCA show that PKS 1622−253 has decreased from 2.5 Jy to 0.9 Jy at 8.640 GHz in the 10 months since 1996 July and has a spectral index of −0.4 between 4.8 and 8.6 GHz ($S_\nu \propto \nu^\alpha$) (Tingay et al. in preparation). The arcsecond-scale radio source is almost unresolved (Perley 1982).

An unresolved optical counterpart has recently been found for this source with a redshift of 0.786 (di Serego Alighieri et al. 1994). Single baseline VLBI observations have been reported by Preston et al. (1985) and Morabito et al. (1986). More recently, simultaneous 2.3 and 8.5 GHz snapshot observations were made with the VLBA in July 1994 by Fey et al. (1996). Model-fitting at both frequencies yielded a compact core with a flux of ∼1.7 Jy.

Figure 3 shows our new VLBA image of PKS 1622−253. The source is dominated by a compact core of 0.6 Jy and 0.6 × 0.5 mas, giving a brightness temperature of $3\times10^{10}$ K at 8.387 GHz. A weak jet-like feature extends approximately 2 mas from the core along a position angle of 306°. This feature may have been too faint for detection with the snapsnot observations of Fey et al. (1996).

### 3.4. PKS 1622−297

PKS 1622−297 is a little studied extragalactic radio source which lies near the direction of the Galactic center ($l$ = 348.8°, $b$ = 13.3°). Mattox et al. (1997a) have summarized the properties of the source at wavelengths other than gamma-ray and also point out the spectacular nature of its gamma-ray emission. PKS 1622−297 is notable as the only known intraday variable in gamma-rays with a gamma-ray burst in 1995 June increasing its flux by a factor of at least 3.6 over a 7.1 hr period, becoming the brightest and most luminous

gamma-ray AGN yet observed with an estimated isotropic luminosity of $2.9\times10^{49}$ ergs $s^{-1}$. Monitoring from the ATCA shows flux density variability at 8.640 GHz on a time-scale of 2 months (the sampling period), indicating shorter time-scale variability. The radio spectrum is complex and inverted between 1.3 and 8.6 GHz (Tingay et al. in preparation). No kpc-scale radio emission has yet been found for this source.

Figure 4 shows the VLBA image of PKS 1622−297 at 1.651 GHz; a strong, slightly extended core component and a one-sided jet is seen. The jet extends to the east at a position angle of 291° and consists of a strong component approximately 15 mas from the core, and a diffuse jet which extends approximately 30 mas from the core. Figure 5 shows the VLBA image at 4.979 GHz, highlighting the bright core and resolving its extension into a separate component approximately 4 mas distant. The diffuse jet is resolved out in this image but the component at 15 mas is still detected weakly. These data were obtained approximately one year before the gamma-ray outburst and it would be interesting to compare these images to post-outburst images, in an attempt to detect any new components created in the outburst.

The radio core brightness temperature for PKS 1622−297 was determined from Figure 5 at 4.979 GHz to be approximately $1\times10^{11}$ K (core flux density of 1.6 Jy and core dimensions of 1.2×0.5 mas).

### 3.5. PKS 1730−130

PKS 1730−130 (NRAO 530) is another low frequency variable radio source (Bondi et al. 1996) at a red shift of z=0.90 which was identified in the second EGRET catalog. Bondi et al. (1996) presents three epochs of VLBI data at 18 cm which shows a north-south source which consists of two components separated by 25 mas. The three epochs span 1980.1 –

1987.9 and no significant structural evolution of the source is seen during this time. Flux density monitoring between 1.3 and 8.6 GHz from the ATCA shows no obvious variability between 1996 July and 1997 February but does show the source to have a strongly inverted spectrum in this frequency range, 5.1 Jy at 1.3 GHz rising to 10.1 Jy at 8.6 GHz (Tingay et al. in preparation).

Figure 6 shows our VLBA image of PKS 1730−130. The source is dominated by a compact core of 8.8 Jy and 0.3 × 0.2 mas, giving a brightness temperature of $2.5\times10^{12}$ K at 8.387 GHz. A jet-like feature extends approximately 5 mas from the core along a position angle of 15°. The component 25 mas from the core which was detected by Bondi et al. (1996) at 18 cm was not detected in Figure 6. This may have been due to a combination of the higher observing frequncy and the subsequently higher resolution (by a factor of three) of the new VLBA data, causing the extended feature to be resolved out. However, the position angle of the pc-scale structure agrees between the two studies. Evolution over the approximately 10 year period may also account for the difference between our image and the data of Bondi et al. (1996).

### 3.6. PKS 1908−201

PKS 1908−201 (OV 213) was not identified with any EGRET source in the first EGRET catalog, but was listed as a positive identification in the second EGRET catalog. Six EGRET observations of the source between 1991 April and 1993 Sep. resulted in a spectral index of 2.5 ± 0.2 being determined. There was no evidence for variability in the gamma ray flux at >95% confidence level. ATCA monitoring observations show that the source is a slow variable at cm wavelengths and has a spectral index of 0.0 between 4.8 and 8.6 GHz (Tingay et al. in preparation). No arcsecond-scale radio structure has been detected for this source.

Trans-continental VLBI observations have detected the source at 2.3 and 8.4 GHz (Preston et al 1985; Morabito et al. 1986) and more recently, PKS 1908−201 was observed as one of the 140 compact sources in the survey of Moellenbrock et al. (1996). On the maximum baseline of 777 M$\lambda$ the source had a correlated flux of 0.75±0.09 Jy, close to the median for the sample, but among the lowest of the 21 EGRET sources in the sample (four of which were marginal detections).

Figure 7 shows the VLBA image of PKS 1908−201, the first VLBI image made of this source. It is dominated by a compact core of 1.3 Jy and 0.7 × 0.2 mas, giving a brightness temperature of $2\times10^{11}$ K at 8.387 GHz. A jet-like feature extends approximately 3 mas from the core along a position angle of 52°.

## 4. DISCUSSION

Mattox et al. (1997b) identify 11 radio sources south of $\delta = -10°$ with a high probability of being counterparts of EGRET sources. This paper completes the VLBI observation of these 11 radio sources. Paper I presented the first results in this study for three sources and this paper has presented the first results for two more as well as four previously observed sources (including one source from Paper I). Three other sources remain in this declination range: the recently identified gamma-ray source, the gravitational lens PKS 1830−211, which has been observed previously with VLBI by Jauncey et al. (1991), Jones et al. (1996), and Lovell et al. (1997); and PKS 1424−418 and PKS 2052−474 which have recently been observed from the Southern Hemisphere (Tingay et al. in preparation). The 11 sources south of $\delta = -10°$ represent over a quarter of the 42 listed by Mattox et al (1997b).

### 4.1. Jet bending and gamma-ray emission

von Montigny et al. (1995) have studied a selection of superluminal blazars and strong flat-spectrum radio sources which have not been detected as gamma-ray sources. They make the interesting observation that 5 of the 8 strong flat-spectrum sources considered in their study showed evidence for having bent or misaligned jets[1], whereas for the 8 identified sources from Phase I EGRET observations with the relevant radio data, 6 had straight jets ($<35°$ misalignment between pc and kpc-scale radio jets).

von Montigny et al. (1995) make the suggestion that if gamma-ray emission originates deep within the jet of an AGN and the jet bends significantly on sub-pc to kpc-scales then it is possible that the gamma-ray emission would be beamed away from our line of sight, while the radio emission could still be beamed along our line of sight by virtue of the jet bending. We would then observe a radio loud, flat-spectrum, but gamma-ray quiet AGN.

Conversely, for jets which do not bend, we can lie within both the gamma-ray and radio beaming cones, allowing us to observe a radio loud, flat-spectrum, gamma-ray loud AGN.

Two other possibilities also exist in this scenario. For bent jets we may lie within the gamma-ray beaming cone but not the radio beaming cone. Observationally such a source might appear as a faint, steep-spectrum, but gamma-ray loud AGN. This possibility is, in general, difficult to distinguish due to the large uncertainties in gamma-ray source positions which can cause a number of candidate identifications to lie within a gamma-ray source

---

[1]5 of 6 really, since they could not find data for two sources, PKS 0438−436 and PKS 0637−752; see Tingay et al. (1997, ApJ, submitted) for VLBI data which shows that PKS 0436−438 is misaligned and PKS 0637−752 is aligned, bringing the von Montigny et al. (1995) statistics to 6 of 8 with bent jets

error circle. Finally, for both bent and straight jets, there may be sources for which we lie in neither the gamma-ray or radio beaming cone, in which case they are not detected in gamma-rays.

Thus, taking a 'unified' approach where every strong, flat-spectrum radio source is a gamma-ray emitter, few which have bent jets would be expected to be detectable gamma-ray sources whereas those which have straight jets would be expected to appear as strong gamma-ray sources. So, is there a preference for the EGRET-identified, radio-loud AGN to have less prominent or less frequent jet bending than similar radio sources which are gamma-ray quiet?

We pursue this question by compiling jet bend data from §3 and the literature for a sample of EGRET-identified sources and a control sample of gamma-ray quiet radio sources, derived from the Pearson-Readhead complete sample of VLBI sources. With these two samples we wish to see if there are any significant differences in the jet bend statistics for EGRET-identified and gamma-ray quiet radio sources.

We note that there exist different opinions in the literature regarding which EGRET sources should be considered to be robust identifications. The lists of robust identifications produced by Mattox et al. (1997b) and Punsley (1997) differ at the 10% level in the number of sources they contain. The list of Mattox et al. (1997b) contains 42 sources and that of Punsley (1997) contains 46 sources. A total of 36 sources are common to the two lists. Here we have chosen the list of Mattox et al. (1997b) to work from since the comparison of the two lists might indicate that only 6/42 in this list are possibly suspect, rather than 10/46 from the list of Punsley (1997). The uncertainty in which sources are considered robustly identified surely underlines the dangers for statistical studies which include sources which have been identified with low confidence only.

Table 3 lists jet bend angle statistics for the 42 EGRET-identified radio sources listed

by Mattox et al. (1997b) and includes bend angle data on the pc-scale jets measured from VLBI images and bend angle data on the kpc-scale from VLA or ATCA observations. Table 4 lists the same information for a sample of radio sources based upon the sample of Pearson and Readhead (1988). Pearson-Readhead sources which were classified as compact sources with flat radio spectra in the range 1 – 10 GHz were selected for the gamma-ray quiet sample, including the objects classified as *compact F double* and *irregular flat-spectrum.* The EGRET-identified sources in the Pearson-Readhead list have been removed from the sample as have two sources which recently have been clearly classified as GHz Peaked-Spectrum radio sources: 1031+567 (Taylor et al. 1996) and 2021+614 (O'Dea et al. 1996). This selection gives us a sample of 26 gamma-ray quiet radio sources with flux densities above 1.3 Jy and with flat radio spectra, intended to be a good match to the radio properties of the 42 EGRET-identified radio sources. Figure 8 shows a comparison of the two samples in the $\log_{10}(S_{5GHz})$ vs spectral index ($S \propto \nu^{\alpha}$) plane using total flux density data from Stickel, Meisenheimer, and Kühr (1994).

Histograms of the spectral index distributions (Figures 9a and 9b) for the two samples show no significant differences. Using a two-sided Komolgorov-Smirnov (K-S) two-sample test, the probability that the null hypothesis holds ($H_o$ is the null hypothesis, the case that the two distributions being compared are not significantly different) is $p(H_o) = 0.99$. Figures 9c and 9d show the red shift distributions for the two samples and again the K-S test shows that the two distributions are likely to have the same parent distribution, $p(H_o) = 0.34$. These tests of the red shift and spectral index distributions show that the two samples are well matched in their basic properties.

Figures 9e and 9f, histograms of the flux density distributions, show a tendency for the EGRET-identified radio sources to have higher 5 GHz flux densities than the gamma-ray quiet radio sources. Using the same K-S test the two distributions are found

to be significantly different, $p(H_o) = 0.02$. Moellenbrock et al. (1996), Impey (1996), and Mattox et al. (1997) have all found similar results for different samples. EGRET-identified radio sources have, on average, higher flux densities than their parent population of bright, flat-spectrum radio sources.

Now, having compared the basic radio properties of the two samples, we can investigate their jet bending properties. In Figures 10a and 10b we plot the distribution of maximum jet bend (the single largest deflection in the jet as can be estimated from radio contour maps) on the pc-scale for the two samples. Using the K-S test, a significant difference was found between the distributions, $p(H_o) = 0.02$. Likewise in Figures 10c and 10d, the distributions for the maximum jet bend on kpc-scales are shown for the two samples. No significant difference was found, $p(H_o) = 0.50$. In Figures 11a and 11b we plot the number of jet bends per source observed on the pc-scale for the two samples. As the K-S test is not appropriate for these data, since they are no longer continuous but discrete data, we use a contigency table chi-squared test (Langley 1970), showing a significant difference, $P(H_o) = 0.01$ ($\chi^2 = 11.4$ with three degrees of freedom). For the distributions of number of bends in the kpc-scale jets, Figures 11c and 11d, $\chi^2 = 0.4$ is found with two degrees of freedom, corresponding to $P(H_o) = 0.82$, showing that the distributions are not significantly different.

Finally, we plot the pc-scale to kpc-scale misalignments for the two samples in Figures 12a and 12b. Again we apply the K-S test (since the data are continuous) and find no reason to reject the null hypothesis, that the two distributions are the same, $p(H_o) = 0.89$. It should be noted here that the pc-scale to kpc-scale misalignment angle tabulated in Tables 3 and 4 and used in Figures 12a and 12b is slightly different to that used in previous studies (Pearson and Readhead 1988; Werhle et al. 1989; Conway and Murphy 1993). We use the difference between the final jet PA on the pc-scale and the initial PA on the kpc-scale, since

we have made an effort to follow jet bending independently for the pc and kpc-scale jets. Bower et al. (1997) have considered the pc to kpc-scale misalignment angle distribution of the EGRET-identified sources in a fashion to compare with the results of Pearson and Readhead (1988) and find no significant difference between the EGRET-identified and gamma-ray quiet sources. A summary of our statistical tests and results is given in Table 5.

Thus, we have considered several statistics describing both the degree and incidence of jet bending on pc and kpc-scales: number of jet bends per source; maximum jet bends; and pc-scale to kpc-scale jet misalignments. We have found evidence to suggest that the jet bending characteristics of EGRET-identified and gamma-ray quiet, flat-spectrum radio sources are significantly different on pc-scales. We found significant differences between the two populations when we considered the number of jet bends per source and the maximum jet bends seen in VLBI images of the pc-scale radio structures of these sources; the gamma-ray quiet sources appear to have more bends per source and a greater tendency for more extreme bending than the EGRET-identified sources, on these scales. No evidence has been found for a significant difference in jet bending properties between the two samples when kpc-scale properties were considered.

On the face of it, this result argues for a clear difference between those sources which produce gamma-rays and those which do not. This difference may be in the physical structure of the jet on pc-scales or in the geometry in which we view the jet (the appearance of jet bending is highly orientation dependent). However, we need to be somewhat careful when interpretating these statistics. In particular, the analysis presented here cannot distinguish between differences which are introduced by observational systematics and real differences. For example, the sample of gamma-ray quiet radio sources is selected from the Pearson-Readhead complete sample. Thus, these sources all lie at relatively high northern declinations and many have been imaged extensively with large VLBI arrays as part of

surveys, as well as with the VLA. These conditions, in general, make for sensitive, robust VLBI images and a certain homogenity of data.

On the other hand, the EGRET-identified sample considered here are scattered over the entire sky and have been imaged using a wide variety of VLBI arrays, observing frequencies, and are often at near-equatorial declinations, where VLBI imaging is more difficult for both northern and southern hemisphere arrays. Under these conditions VLBI images tend to be less sensitive and robust, and less detailed. The data set as a whole is certainly less homogeneous. It is therefore possible that, on average, VLBI images of the EGRET-identified radio sources are less representitive of their real structure than the VLBI images of the gamma-ray quiet radio sources. Unfortunately this statement is very difficult to quantify from a set of contour maps but it is concievable that these observational effects could mean the difference between a significant result and an insignificant result in our statistics. Until truly homogeneous data for a sample of EGRET-identified radio sources can be obtained, this uncertainty cannot be resolved with high confidence.

If true, and confirmed by future investigations, the tentative results of this paper support the suggestion of von Montigny et al. (1995) that EGRET-identified AGN have preferentially straight jets and gamma-ray quiet AGN have bent jets. This could be an important clue with which we can probe the origin of the differences between gamma-ray loud and quiet AGN. Perhaps the beaming arguement is correct, that we lie outside the gamma-ray beaming cone, for gamma-ray quiet sources, by virtue of jet bending. An alternative hypothesis could be that gamma-ray emission is suppressed somehow if the jet is disrupted close to the nucleus, as evidenced by bending on small scales.

The significant difference found between the 5 GHz flux density distributions is consistent with the results of previous investigations and may also offer a hint as to the difference between EGRET-identified and gamma-ray quiet AGN. The higher radio flux

density of EGRET-identified sources may be an effect of beaming, due to more highly aligned and/or faster jets in the EGRET-identified sources, or conversely may be an intrinsic effect, indicating that the central engines in the EGRET-identified sources are currently experiencing an outburst, perhaps due to being actively fuelled. In this case multi-epoch VLBI observations and multi-wavelength monitoring might reveal the ejection of new jet components following outbursts. A good candidate source for these types of observations would be PKS 1622−297.

## 5. SUMMARY

We have presented VLBA observations of 6 EGRET-identified compact radio sources in the Southern Hemisphere, following on from the results of Paper I. All of the EGRET-identifed sources south of $-10°$ have now been observed with imaging VLBI on at least one occasion. For one of the sources observed here, PKS 0521-365, we tentatively suggest that the pc-scale jet is apparently superluminal.

We have investigated the possibility, suggested by von Montigny et al. (1995), that gamma-ray quiet radio sources have a tendency for more pronounced jet bending than EGRET-identified radio sources, and find evidence supporting the suggestion in VLBI observations of pc-scale jets. However, the interpretation of this result needs to recognise the possibility that systematic differences between the samples, due to observational biases, may have been introduced. We also find a significant difference between the radio flux densities of gamma-ray quiet and EGRET-identified radio sources, consistent with the findings of Moellenbrock et al. (1996), Impey (1996), Mattox et al. (1997b), and Zhou et al. (1997).

The Very Long Baseline Array (VLBA) and the Astronomical Image Processing

Software (AIPS) is developed and maintained by the National Radio Astronomy Observatory which is operated by Associated Universities, Inc., under cooperative agreement with the National Science Foundation. Part of this work was carried out at the Jet Propulsion Laboratory, California Institue of Technology, under contract with the National Aeronautics and Space Administration, and was undertaken while S.J.T. held an NRC – JPL/NASA Research Associateship.

## REFERENCES

Antonucci, R.R.J. & Ulvestad, J.S. 1985, ApJ, 294, 158

Biretta, J.A. & Cohen, M.H. 1987, in Superluminal Radio Sources, Eds. J.A. Zensus & T.J. Pearson (Cambridge: CUP), 40

Bondi, M. et al. 1996, A&A, 308, 415

Bower, G.C. et al. 1997, ApJ, 484, 118

Bridle, A.H., Hough, D.H., Lonsdale, C.J., Burns, J.O., & Laing, R.A. 1994, AJ, 108, 766

Browne, I.A. 1987, in Superluminal Radio Sources, Eds. J.A. Zensus & T.J. Pearson (Cambridge: CUP), 129

Cawthorne, T.V., Wardle, J.F.C., Roberts, D.H., Gabuzda, D.C., & Brown, L.F. 1993, ApJ, 416, 496

Comastri, A., Fossati, G., Ghisellini, G., & Silvano, M. 1997, ApJ, 480, 534

Conway, J.E. & Murphy, D.W. 1993, ApJ, 411, 89

Davis, R.J., Muxlow, T.W.B., & Conway, R.G. 1985, Nature, 318, 343

Dondi, L. & Ghisellini, G. 1995, MNRAS, 273, 583

de Pater, I. & Perley, R.A. 1983, ApJ, 273, 64

di Serego Alighieri, S., Danziger, I.J., Morganti, R., & Tadhunter, C.N. 1994, MNRAS, 269, 998

Fey, A.L., Clegg, A.W., & Fomalont, E.B. 1996, ApJS, 468, 543

Fichtel, C.E. et al. 1994, ApJS, 94, 551

Gabuzda, D.C. & Cawthorne, T.V. 1996 MNRAS, 283, 759

Gabuzda, D.C., Wardle, J.F.C., Roberts, D.H., Aller, M.F., & Aller, H.D. 1994, ApJ, 435, 128

Griffith, M.R, Wright, A.E., Burke, B.F., & Ekers, R.D. 1994, ApJS, 90, 179

Hooimeyer, J.R.A., Schilizzi, R.T., Miley, G.K., & Barthel, P.D. 1992, A&A, 261, 5

Impey, C. 1996, AJ, 112, 2667

Jauncey, D.L. et al. 1991, Nature, 352, 132

Jones, D.L. et al. 1996, ApJ, 470, L23

Jones, D.L., Bääth, L.B., Davis, M.M., & Unwin, S.C. 1984, ApJ, 284, 60

Krichbaum, T.P. et al. 1990, A&A, 230, 271

Langley, R. in Practical Statistics (Dover: New York), pp 269

Lin, Y.C. et al. 1995, ApJ, 442, 96

Lovell, J.E.J. et al. 1996, ApJ, 472, L5

Mattox, J.R. et al. 1997a, ApJ, 476, 692

Mattox, J.R., Schachter, J., Molnar, L., Hartman, R.C., & Patnaik, A.R. 1997b, ApJ, 481, 95

McHardy, I.M., Marscher, A.P., Gear, W.K., Muxlow, T., Lehto, H.J., & Abraham, R.G. 1990, MNRAS, 246, 305

Moellenbrock, G.A. et al. 1996, AJ, 111, 2174

Morabito, D.D., Preston, R.A., Linfield, R.P., Slade, M.A., & Jauncey, D.L. 1986, AJ, 92, 546

Murphy, D.W., Browne, I.A., & Perley, R.A. 1993, MNRAS, 264, 298

Neff, S.G., Roberts, L., & Hutchings, J.B. 1995, ApJS, 99, 349

Nolan, P.L. et al. 1996, ApJ, 459, 100

O'Dea, C.P., Stanghellini, C., Baum, S.A., & Charlot, S. 1996, ApJ, 470, 806

Pauliny-Toth, I.I.K. et al. 1987, Nature, 328, 778

Pearson, T.J. & Readhead, A.C.S. 1988, ApJ, 328, 114

Perley, R.A. 1982, AJ, 87, 859

Perlman, E.S. & Stocke, J.T. 1994, ApJ, 108, 56

Pohl, M. et al. 1995, A&A, 303, 383

Polatitis, A.G. et al. 1995, ApJS, 98, 1

Preston, R.A., Morabito, D.D., Williams, J.G., Faulkner, J., Jauncey, D.L., & Nicolson, G. 1985, AJ, 90, 1599

Preston, R.A. et al. 1989, AJ, 98, 1

Price, R., Gower, A.C., Hutchings, J.B., Talon, S., Duncan, D., & Ross, G. 1993, ApJS, 86, 365

Punsley, B. 1997, AJ, 114, 544

Romanova, M.M. & Lovelace, R.V.E. 1997, ApJ, 475, 97

Saikia, D.J., Wiita, P.J., & Muxlow, T.W.B. 1993, AJ, 105 1658

Salamon, M. & Stecker, F.W. 1994, ApJ, 430, L21

Shepherd, M.C., Pearson, T.J., & Taylor, G.B. 1994, BAAS, 26, 987

Stickel, M., Meisenheimer, K., & Kühr, H. 1994, A&AS, 105, 211

Taylor, G.B., Readhead, A.C.S., & Pearson, T.J. 1996, ApJ, 463, 95

Thompson, D.J. et al. 1995, ApJS, 101, 259

Tingay, S.J. et al. 1996 ApJ 464, 170

Unwin, S.C., Cohen, M.H., Biretta, J.A., Hodges, M.W., & Zensus, J.A. 1989, ApJ, 340, 117

Vermuelen, R.C. & Cohen, M.H. 1994, ApJ, 430, 467

Vermuelen, R.C., Readhead, A.C.S., & Backer, D.C. 1994, ApJ, 430, L41

von Montigny, C. et al. 1995, A&A, 299, 680

Wehrle, A.E. & Cohen, M.H. 1989, ApJ, 346, L69

Wehrle, A.E. et al. 1992, ApJ, 391, 589

Witzel, A. et al. 1988, A&A, 206, 245

Witzel, A. 1987 in Superluminal Radio Sources, Eds. J.A. Zensus & T.J. Pearson (Cambridge: CUP), 83

Wrobel, J.M. 1987 in Superluminal Radio Sources, Eds. J.A. Zensus & T.J. Pearson (Cambridge: CUP), 186

Xu, W., Readhead, A.C.S., Pearson, T.J., Polatidis, A.G., & Wilkinson, P.N. 1995, ApJS, 99, 297

Zensus, J.A., Unwin, S.C., Cohen, M.H., & Biretta, J.A. 1990, AJ, 100, 1777

Zhang, F.J. & Bååth, L.B. 1990, A&A, 236, 47

Zhou, Y.Y. Lu, Y.J., Wang, T.G., Yu, K.N., and Young, E.C.M. 1997, ApJ, 484, L47

---

This manuscript was prepared with the AAS LaTeX macros v4.0.

## TABLE CAPTIONS

**Table 1.** The observation log for VLBA observations of the 6 EGRET-identified radio sources.

**Table 2.** Model-fit parameters for PKS 0521−365, for the observations of 1997 Feb. 17: S is the component flux density in Jy; R is the distance from the component to the core (fixed at R=0); PA is the position angle of the component relative to the core (fixed at PA=0); a is the semi-major axis (FWHM) of the Gaussian component; b/a is the semi-minor to semi-major axis ratio for the Gaussian component; and $\phi$ is the position angle of the component semi-major axis.

**Table 3.** Jet bend data compiled for the 42 AGN listed by Mattox et al. (1997b) as robust identifications. $\phi$ is the radio jet position angle, listed for both the pc and kpc-scales, measured from radio maps. Entries with several values separated with slashes signify those sources with measurable bends; the initial value given is the PA of the jet closest to the core and each subsequent value should be added to the previous value to find the PA of the tangent to the jet. Entries enclosed by brackets signify that the determination of PA is ambiguous and both possibilities are listed but not used in the analysis. $N$ is the number of jet bends in the jet, listed for the pc and kpc scales. $|\theta|_{max}$ is the maximum jet bend angle determined, listed for both the pc and kpc-scales. $\phi_{kpc,i} - \phi_{pc,f}$ is the difference between the *final* pc-scale jet PA and the *initial* kpc-scale jet PA. * PKS 1830−211 was not used in the analysis due to its unusual classification as a gravitational lens.

**Table 4.** Jet bend angle data compiled from the literature for a sample of 26 sources derived from the Pearson-Readhead sample (see text). Parameters are identical to Table 3. References for Tables 3 and 4 follow: 1. Bondi et al. 1996, 2. Tingay et al. 1996, 3. Murphy, Browne, & Perley 1993, 4. Jones et al. 1984, 5. Antonucci & Ulvestad 1985, 6. Wehrle et al. 1992, 7. Perley 1982, 8. Pohl et al., 9. Polatitis et al. 1995, 10. Gabuzda et al. 1994, 11. Price et al. 1993, 12. Kritchbaum et al. 1990, 13. Conway & Murphy 1993, 14. Zhang & Baath 1990, 15. McHardy et al. 1990, 16. Hooimeyer et al. 1992, 17. Saikia et al. 1993, 18. Zensus et al. 1990, 19. Davis, Muxlow, & Conway 1985, 20. Unwin et al. 1989, 21. de Pater & Perley, 22. this paper, 23. Lovell 1997, private communication, 24. Wehrle & Cohen 1989, 25. Pauliny-Toth et al. 1987, 26. Xu et al. 1995, 27. Witzel et al. 1988, 28. Browne 1987, 29. Biretta & Cohen 1987, 30. Witzel 1987, 31. Wrobel 1987, 32. Preston et al. 1989, 33. Jauncey et al. 1991, 34. Pearson & Readhead 1988, 35. Perlman et al. 1994, 36. Vermuelen, Readhead, & Backer 1994, 37. Bridle et al. 1994, 38. Neff, Roberts, & Hutchings 1995, 39. Gabuzda & Cawthorne 1996, 40. Cawthorne et al. 1993

**Table 5.** Summary of statistical tests and results. For a result to be considered significant the probability that the null hypothesis (that the EGRET-identified and gamma-ray quiet sources have the same properties) holds must be less than 0.05 (95% confidence level).

## FIGURE CAPTIONS

**Figure 1** VLBA image of PKS 0521−365 at 8.387 GHz from 1997 Feb. 17. Contour levels are -0.25, 0.25, 0.5, 1, 2, 4, 8, 16, 32, and 64% of the peak flux density of 1.5 Jy/beam. Beam FWHM, 7.1×2.4 mas at 2.°0.

**Figure 2** VLBA image of PKS 1127−145 at 8.387 GHz from 1997 Feb. 17. Contour levels are -0.5, 0.5, 1, 2, 4, 8, 16, 32, and 64% of the peak flux density of 1.4 Jy/beam. Beam FWHM, 4.4×1.9 mas at −4.°1.

**Figure 3** VLBA image of PKS 1622−253 at 8.387 GHz from 1997 Feb. 17. Contour levels are -1, 1, 2, 4, 8, 16, 32, and 64% of the peak flux density of 0.5 Jy/beam. Beam FWHM, 1.8×0.7 mas at −3.°8.

**Figure 4** VLBA image of PKS 1622−297 at 1.651 GHz from 1994 Sep. 1. Contour levels are -1, 1, 2, 4, 8, 16, 32, and 64% of the peak flux density of 0.8 Jy/beam. Beam FWHM, 9.9×3.3 mas at 1.°4.

**Figure 5** VLBA image of PKS 1622−297 at 4.979 GHz from 1994 Aug. 23. Contour levels are -1, 1, 2, 4, 8, 16, 32, and 64% of the peak flux density of 1.3 Jy/beam. Beam FWHM, 4.1×1.3 mas at −2.°1.

**Figure 6** VLBA image of PKS 1730−130 at 8.387 GHz from 1997 Feb. 17. Contour levels are -0.25, 0.25, 0.5, 1, 2, 4, 8, 16, 32, and 64% of the peak flux density of 8.3 Jy/beam. Beam FWHM, 1.8×0.7 mas at −5.°1.

**Figure 7** VLBA image of PKS 1908−201 at 8.387 GHz from 1997 Feb. 17. Contour levels

are 1, 2, 4, 8, 16, 32, and 64% of the peak flux density of 1.1 Jy/beam. Beam FWHM, 1.8×0.7 mas at −3.°5.

**Figure 8** EGRET-identified (crosses) and gamma-ray quiet (stars) from the two samples plotted in the $\log_{10}(S_{5GHz})$ vs spectral index plane. Data are from Stickel, Kühr and Misenheimer (1994).

**Figure 9** Top panel: distributions of spectral index for EGRET-identified (9a) and gamma-ray quiet (9b) radio sources from the two samples. Middle panel: distributions of red shift for EGRET-identified (9c) and gamma-ray quiet (9d) radio sources from the two samples. Lower panel: distributions of $\log_{10}$(5 GHz flux density) for EGRET-identified (9e) and gamma-ray quiet (9f) radio sources from the two samples.

**Figure 10** Top panel: distributions of maximum pc-scale jet bend for EGRET-identified (10a) and gamma-ray quiet (10b) radio sources from the two samples. Lower panel: distributions of maximum kpc-scale jet bend for EGRET-identified (10c) and gamma-ray quiet (10d) radio sources from the two samples.

**Figure 11** Top panel: distributions of number of pc-scale jet bends for EGRET-identified (11a) and gamma-ray quiet (11b) radio sources from the two samples. Lower panel: distributions of number of kpc-scale jet bends for EGRET-identified (11c) and gamma-ray quiet (11d) radio sources from the two samples.

**Figure 12** Distributions of pc-scale to kpc-scale jet misalignments for EGRET-identified (12a) and gamma-ray quiet (12b) radio sources from the two samples.

| Source | Epoch | Frequency (GHz) |
|---|---|---|
| PKS 0521−365..... | 1997 Feb. 17 | 8.387 |
| PKS 1127−145..... | 1997 Feb. 17 | 8.387 |
| PKS 1622−253..... | 1997 Feb. 17 | 8.387 |
| PKS 1622−297..... | 1994 Sep. 01 | 1.651 |
| PKS 1622−297..... | 1994 Aug. 23 | 4.979 |
| PKS 1730−130..... | 1997 Feb. 17 | 8.387 |
| PKS 1908−201..... | 1997 Feb. 17 | 8.387 |

Table 1:

| S (Jy) | R (mas) | PA° | a (mas) | b/a | $\phi$ |
|---|---|---|---|---|---|
| 1.65 | 0.00 | 0.0 | 1.16 | 0.63 | 126.1 |
| 0.09 | 3.09 | 304.0 | 2.03 | 0.31 | 14.4 |
| 0.10 | 10.89 | 316.3 | 7.46 | 0.00 | 116.9 |
| 0.02 | 18.78 | 312.4 | 2.17 | 0.38 | 156.0 |
| 0.16 | 26.99 | 312.1 | 7.01 | 0.39 | 148.8 |

Table 2:

| SOURCE | z | $\phi_{pc}$ | $N_{pc}$ | $\|\theta_{pc}\|_{max}$ | $\phi_{kpc}$ | $N_{kpc}$ | $\|\theta_{kpc}\|_{max}$ | $\phi_{kpc,i} - \phi_{pc,f}$ | REFS |
|---|---|---|---|---|---|---|---|---|---|
| 0202+149 | 1.202 | 289 | 0 | 0 | - | - | - | - | 1 |
| 0208−512 | 1.003 | 233 | 0 | 0 | 219 | 0 | 0 | 14 | 2 |
| 0234+285 | 1.213 | 345 | 0 | 0 | 0/-47 | 1 | 47 | 15 | 3,6 |
| 0235+164 | 0.940 | 7 | 0 | 0 | 332/22 | 1 | 22 | 35 | 3,4 |
| 0336−019 | 0.852 | 65 | 0 | 0 | 345 | 0 | 0 | 80 | 6 |
| 0420−014 | 0.915 | 0 | 0 | 0 | - | - | - | - | 6 |
| 0440−003 | 0.844 | - | - | - | 100 | 0 | 0 | - | 11 |
| 0458−020 | 2.286 | 305 | 0 | 0 | 237 | 0 | 0 | 68 | 6 |
| 0521−365 | 0.055 | 310 | 0 | 0 | 312/−11 | 1 | 11 | 2 | 2 |
| 0528+134 | 2.060 | 50/−41 | 1 | 41 | 0 | 0 | 0 | 9 | 7,8 |
| 0537−441 | 0.894 | 3 | 0 | 0 | 305 | 0 | 0 | 58 | 2 |
| 0716+714 | - | 18 | 0 | 0 | 300 | 0 | 0 | 78 | 9,7 |
| 0735+178 | >0.424 | 55 | 0 | 0 | 160 | 0 | 0 | 105 | 3,10 |
| 0827+243 | 2.046 | - | - | - | 199 | 0 | 0 | - | 11 |
| 0829+046 | 0.180 | - | - | - | 220/90 | 1 | 90 | - | 5 |
| 0836+710 | 2.172 | 220 | 0 | 0 | 212 | 0 | 0 | 8 | 3,12 |
| 0954+556 | 0.909 | - | - | - | 297 | 0 | 0 | - | 3 |
| 0954+658 | 0.368 | 306 | 0 | 0 | 203 | 0 | 0 | 103 | 13 |
| 1101+384 | 0.031 | 316 | 0 | 0 | 301 | 0 | 0 | 15 | 14 |
| 1127−145 | 1.187 | 81/−29 | 1 | 29 | 41 | 0 | 0 | 11 | 6 |
| 1156+295 | 0.729 | 24 | 0 | 0 | 343/60 | 1 | 60 | 41 | 15 |
| 1219+285 | 0.102 | 100 | 0 | 0 | 246 | 0 | 0 | 142 | 35,39 |
| 1222+216 | 0.435 | 346 | 0 | 0 | 24/90/−90 | 2 | 90 | 38 | 16,17 |
| 1226+023 | 0.158 | 232 | 0 | 0 | 230/−12 | 1 | 12 | 2 | 18,19 |
| 1253−055 | 0.538 | 215 | 0 | 0 | 207/−8 | 1 | 8 | 8 | 20,21 |
| 1406−076 | 1.494 | - | - | - | - | - | - | - | - |
| 1424−418 | 1.522 | 56 | 0 | 0 | -10 | 0 | 0 | 66 | 32 |

| SOURCE | z | $\phi_{pc}$ | $N_{pc}$ | $\|\theta_{pc}\|_{max}$ | $\phi_{kpc}$ | $N_{kpc}$ | $\|\theta_{kpc}\|_{max}$ | $\phi_{kpc,i} - \phi_{pc,f}$ | REFS |
|---|---|---|---|---|---|---|---|---|---|
| 1510−089 | 0.360 | 193 | 0 | 0 | 163 | 0 | 0 | 30 | 1,11 |
| 1606+106 | 1.226 | - | - | - | 270 | 0 | 0 | - | 3, |
| 1611+343 | 1.401 | 154 | 0 | 0 | - | - | - | - | 1 |
| 1622−253 | 0.786 | 308 | 0 | 0 | 303 | 0 | 0 | 5 | 7,22 |
| 1622−297 | 0.815 | 292 | 0 | 0 | - | - | - | - | 22 |
| 1633+382 | 1.814 | 296 | 0 | 0 | 168 | 0 | 0 | 128 | 13 |
| 1730−130 | 0.902 | 0 | 0 | 0 | 273 | 0 | 0 | 87 | 1,7 |
| 1739+522 | 1.375 | 319 | 0 | 0 | 260 | 0 | 0 | 59 | 13 |
| 1830−210* | - | - | - | - | - | - | - | - | 33 |
| 1908−201 | - | 37 | 0 | 0 | - | - | - | - | 22 |
| 2052−474 | 1.489 | - | - | - | 214 | 0 | 0 | - | 23 |
| 2200+420 | 0.069 | 185 | 0 | 0 | - | - | - | - | 9 |
| 2209+236 | 1.489 | - | - | - | - | - | - | - | - |
| 2230+114 | 1.037 | 159/−71 | 1 | 71 | 147 | 0 | 0 | 59 | 5,24 |
| 2251+158 | 0.859 | 253/47 | 1 | 47 | 299/17 | 0 | 0 | 1 | 3,25 |

Table 3: Continues from previous page

| SOURCE | z | $\phi_{pc}$ | $N_{pc}$ | $\|\theta_{pc}\|_{max}$ | $\phi_{kpc}$ | $N_{kpc}$ | $\|\theta_{kpc}\|_{max}$ | $\phi_{kpc,i} - \phi_{pc,f}$ | REFS |
|---|---|---|---|---|---|---|---|---|---|
| 0016+731 | 1.781 | 180 | 0 | 0 | 270 | 0 | 0 | 90 | 7,40 |
| 0133+476 | 0.859 | 355 | 0 | 0 | - | - | - | - | 9 |
| 0153+744 | 2.338 | 114/31/53 | 2 | 53 | - | - | - | - | 27 |
| 0212+735 | 2.367 | 99/-19 | 1 | 19 | - | - | - | - | 27 |
| 0316+413 | 0.017 | 180 | 0 | 0 | 160/75 | 1 | 75 | 20 | 36,37 |
| 0454+844 | 0.112 | 142/27 | 1 | 27 | - | - | - | - | 39 |
| 0711+356 | 1.62 | - | - | - | 143 | 0 | 0 | - | 3 |
| 0804+499 | 1.43 | 85/87 | 1 | 87 | 201 | 0 | 0 | 29 | 3,9 |
| 0814+425 | 0.026 | 103 | 0 | 0 | 45/-128 | 1 | 128 | 58 | 3,9 |
| 0831+557 | 0.240 | 316/17 | 1 | 17 | 170 | 0 | 0 | 163 | 9,38 |
| 0850+581 | 1.322 | 150 | 0 | 0 | 151/12/-38 | 2 | 38 | 1 | 9,28 |
| 0859+470 | 1.462 | 0/-31 | 1 | 31 | 335 | 0 | 0 | 6 | 3,9 |
| 0923+392 | 0.699 | 109/-90 | 1 | 90 | 76 | 0 | 0 | 57 | 3,9 |
| 0945+408 | 1.252 | 112/-20 | 1 | 20 | 32 | 0 | 0 | 62 | 3,9 |
| 1624+416 | 2.55 | 344/21 | 1 | 21 | 351 | 0 | 0 | 14 | 9,34 |
| 1637+574 | 0.745 | 10 | 0 | 0 | 326/-73 | 1 | 73 | 44 | 3,26 |
| 1641+399 | 0.595 | 275/26 | 1 | 26 | 328 | 0 | 0 | 27 | 3,29 |
| 1642+690 | 0.751 | 196 | 0 | 0 | 170 | 0 | 0 | 26 | 3,9 |
| 1652+398 | 0.0377 | 110/−66 | 1 | 66 | 45 | 0 | 0 | 1 | 9,26 |
| 1749+701 | 0.77 | 5 | 0 | 0 | 21 | 0 | 0 | 16 | 9,26 |
| 1803+784 | 0.68 | 268 | 0 | 0 | 193 | 0 | 0 | 75 | 3,30 |
| 1807+698 | 0.050 | 259 | 0 | 0 | 244/24 | 1 | 24 | 9 | 9,31 |
| 1823+568 | 0.664 | 198/-9 | 1 | 9 | 95 | 0 | 0 | 94 | 3,9 |
| 1928+738 | 0.302 | 164/8/-29/41 | 3 | 41 | 195/-55 | 1 | 55 | 11 | 3,27 |
| 1954+513 | 1.22 | 283 | 0 | 0 | 350 | 0 | 0 | 56 | 9,26 |
| 2351+456 | 2.0 | 321 | 0 | 0 | 25/75 | 1 | 75 | 54 | 9,39 |

Table 4:

| Source Property | Statistical test | $p(H_0)$ | Significant |
|---|---|---|---|
| Spectral index | K-S | 0.99 | no |
| Redshift | K-S | 0.34 | no |
| Total 5 GHz flux density | K-S | 0.02 | yes |
| Maximum jet bend (pc) | K-S | 0.02 | yes |
| Maximum jet bend (kpc) | K-S | 0.50 | no |
| Number of jet bends (pc) | $\chi^2$ | 0.01 | yes |
| Number of jet bends (kpc) | $\chi^2$ | 0.82 | no |
| pc to kpc misalignment | K-S | 0.89 | no |

Table 5:

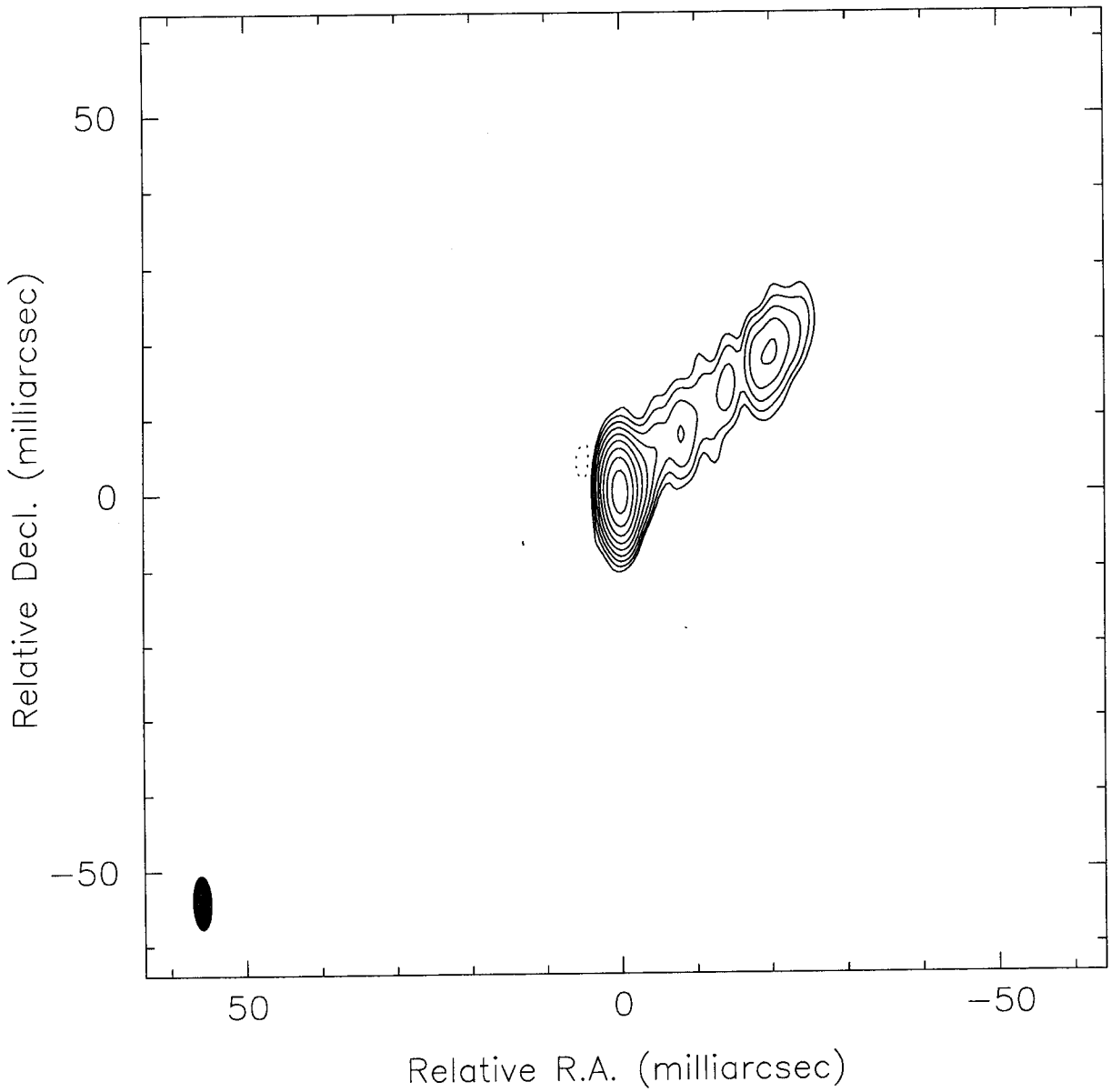
50
0
−50
Relative Decl. (milliarcsec)
50
0
−50
Relative R.A. (milliarcsec)

Fig. 1.—

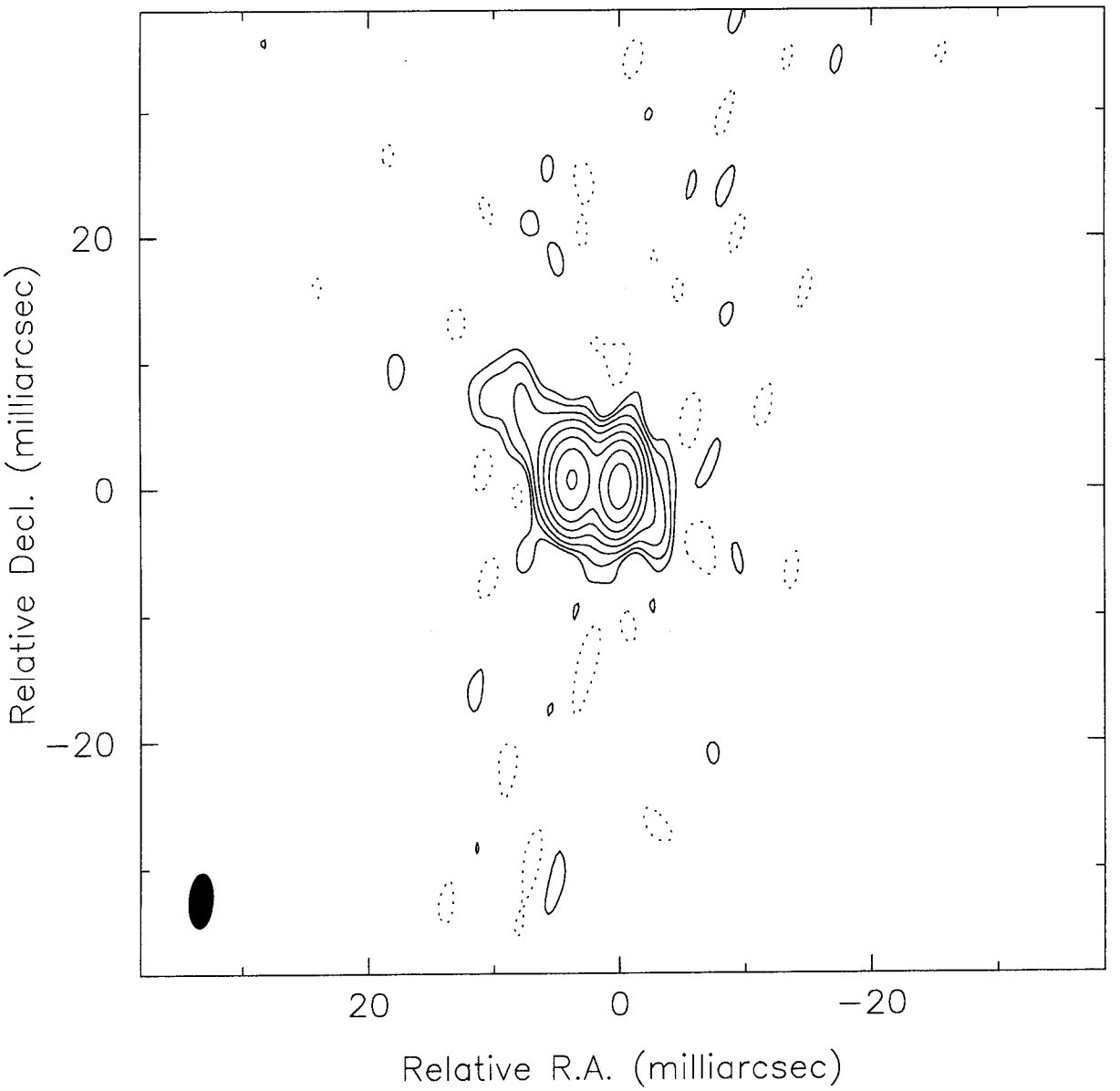
20
0
−20
Relative Decl. (milliarcsec)
20
0
−20
Relative R.A. (milliarcsec)

Fig. 2.—

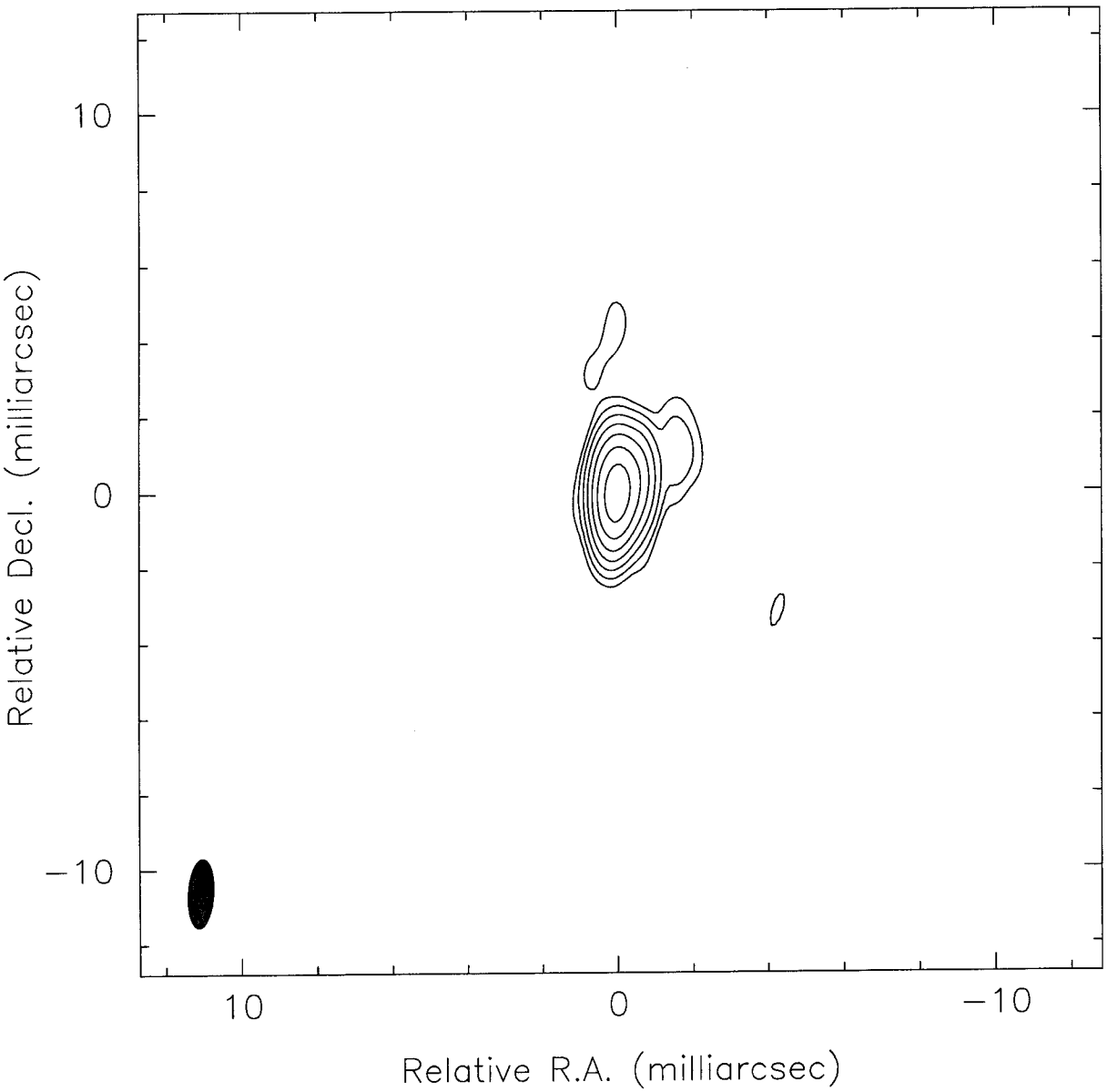
10
0
−10
Relative Decl. (milliarcsec)
10
0
−10
Relative R.A. (milliarcsec)

Fig. 3.—

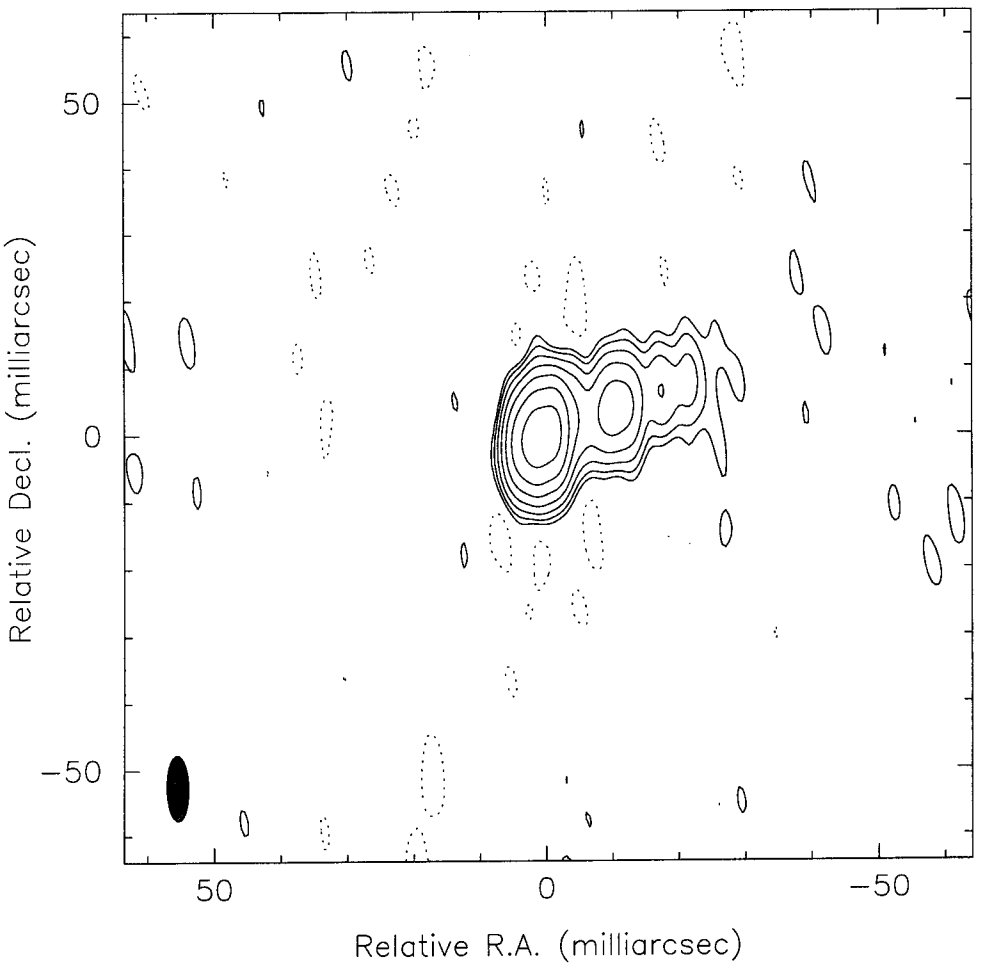
50
0
−50
Relative Decl. (milliarcsec)
50
0
−50
Relative R.A. (milliarcsec)

Fig. 4.—

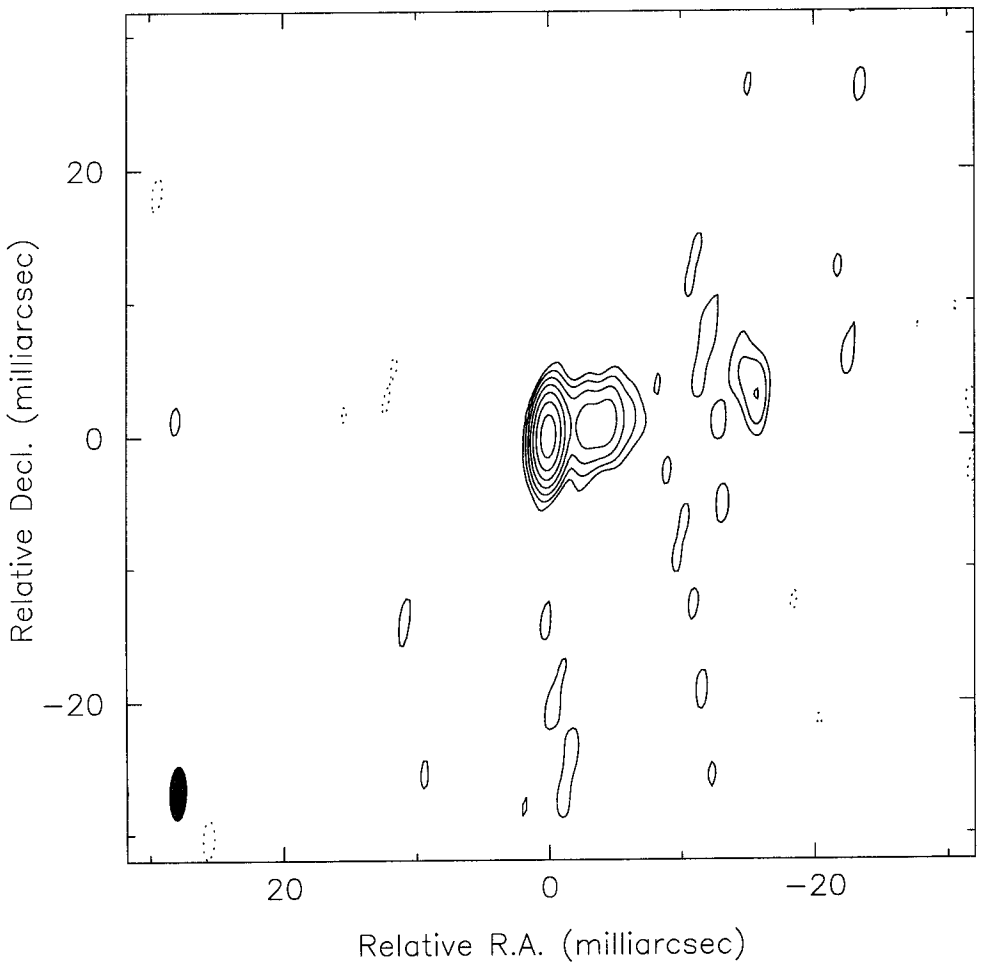
20
0
−20
Relative Decl. (milliarcsec)
20
0
−20
Relative R.A. (milliarcsec)

Fig. 5.—

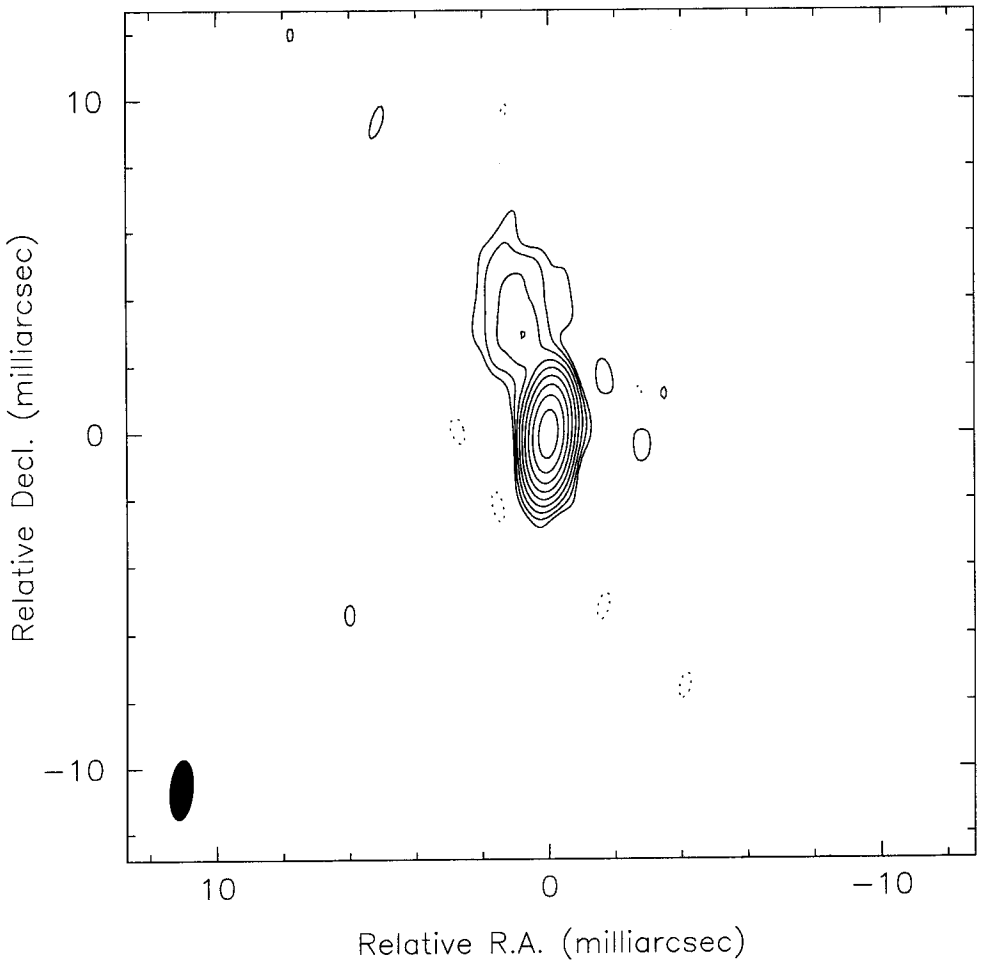
10
0
−10
Relative Decl. (milliarcsec)
10
0
−10
Relative R.A. (milliarcsec)

Fig. 6.—

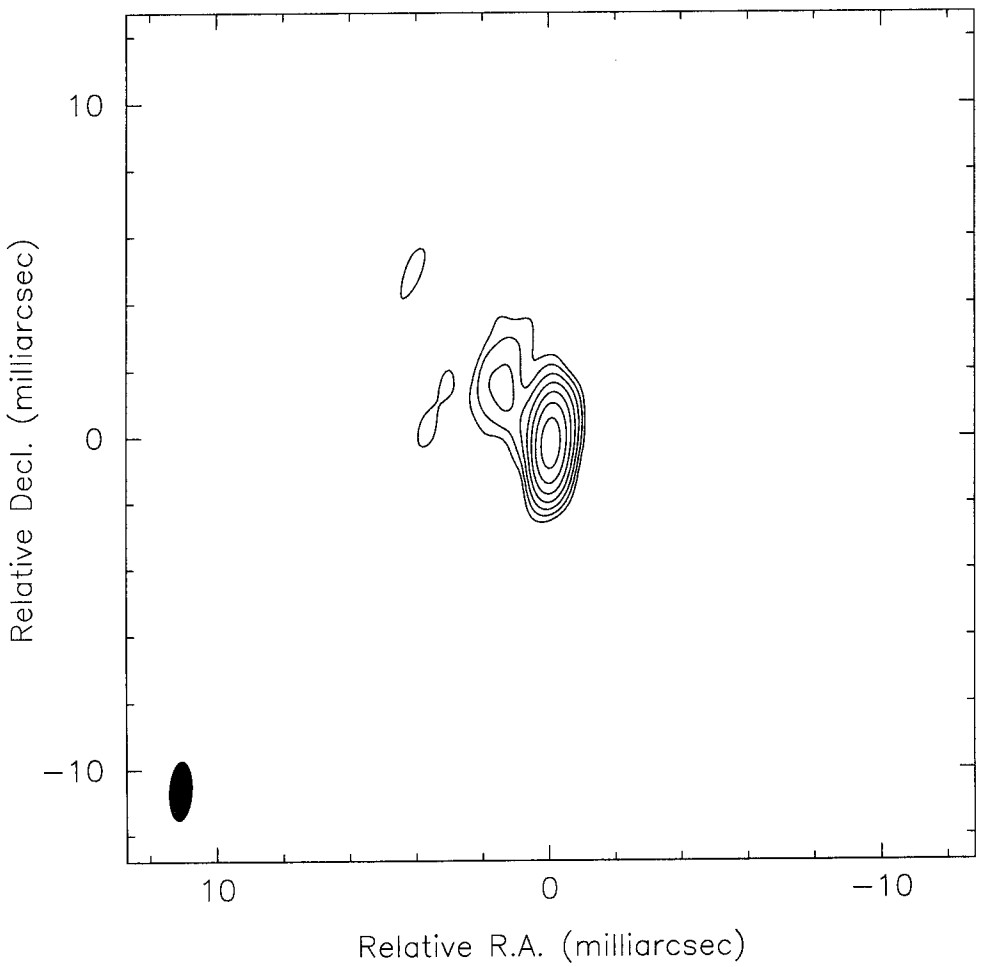
10
0
−10
Relative Decl. (milliarcsec)
10
0
−10
Relative R.A. (milliarcsec)

Fig. 7.—

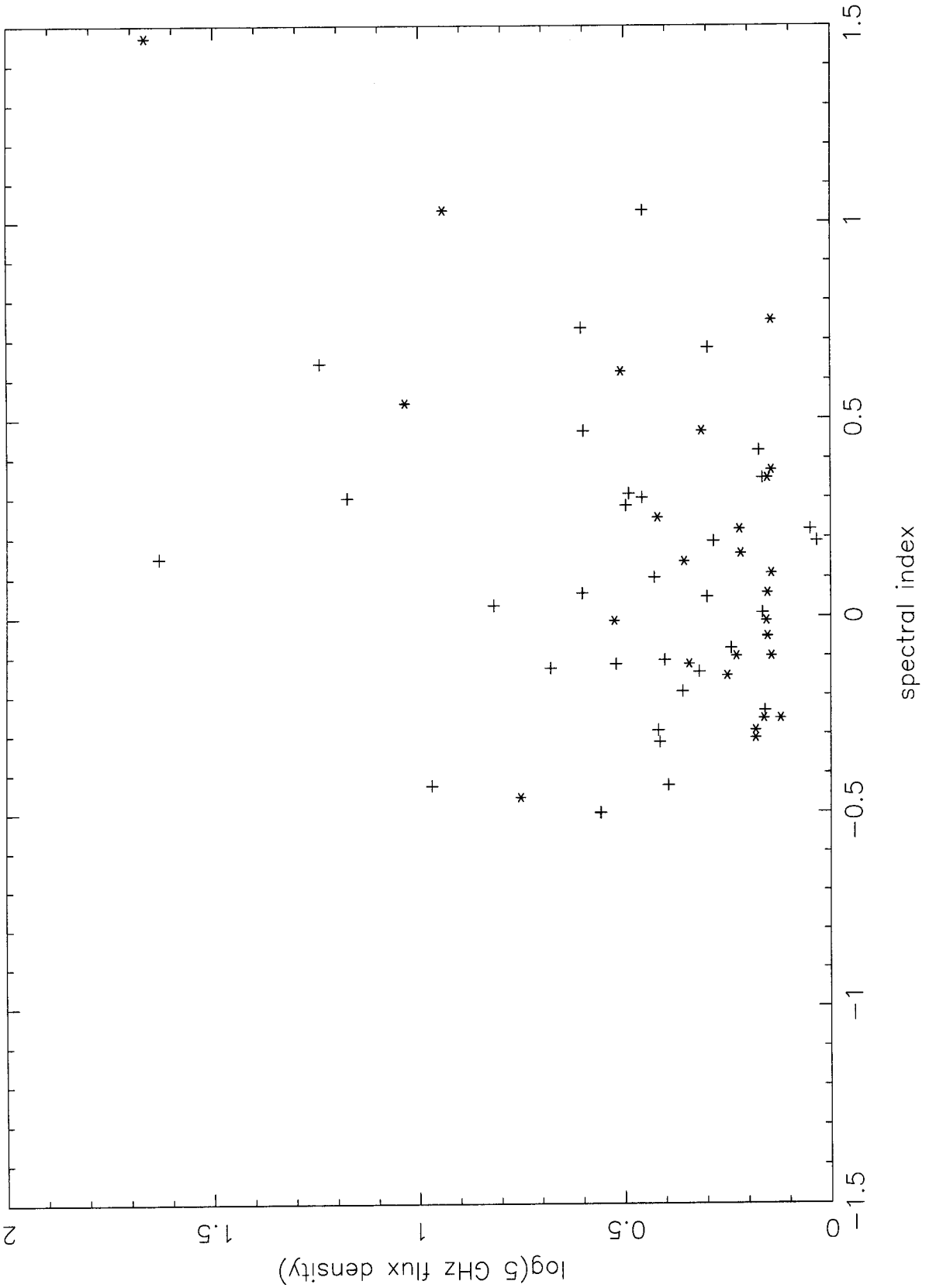


Fig. 8.—

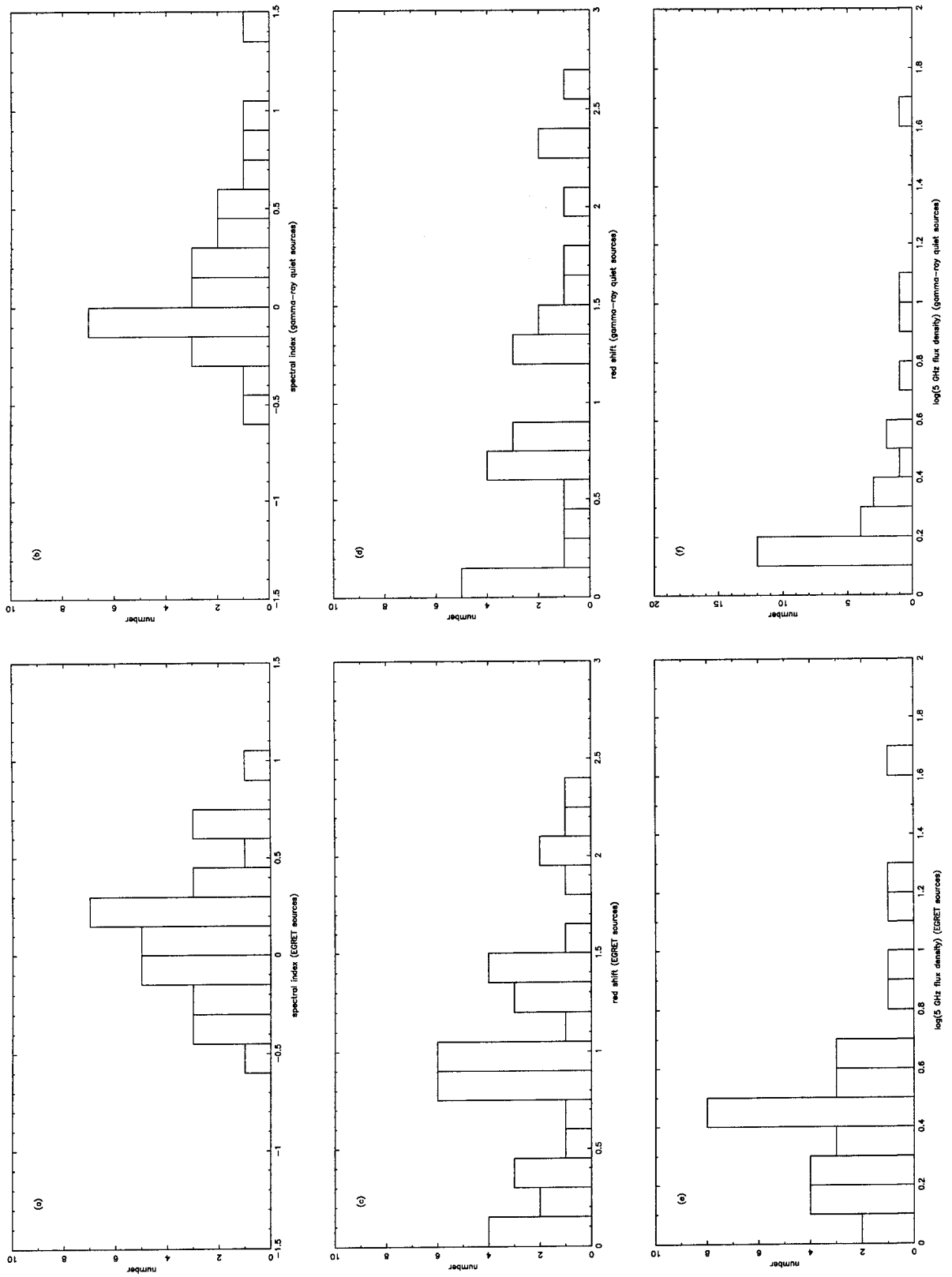
(a)
number
spectral index (EGRET sources)
(b)
number
spectral index (gamma-ray quiet sources)
(c)
number
red shift (EGRET sources)
(d)
number
red shift (gamma-ray quiet sources)
(e)
number
log(5 GHz flux density) (EGRET sources)
(f)
number
log(5 GHz flux density) (gamma-ray quiet sources)

Fig. 9.—

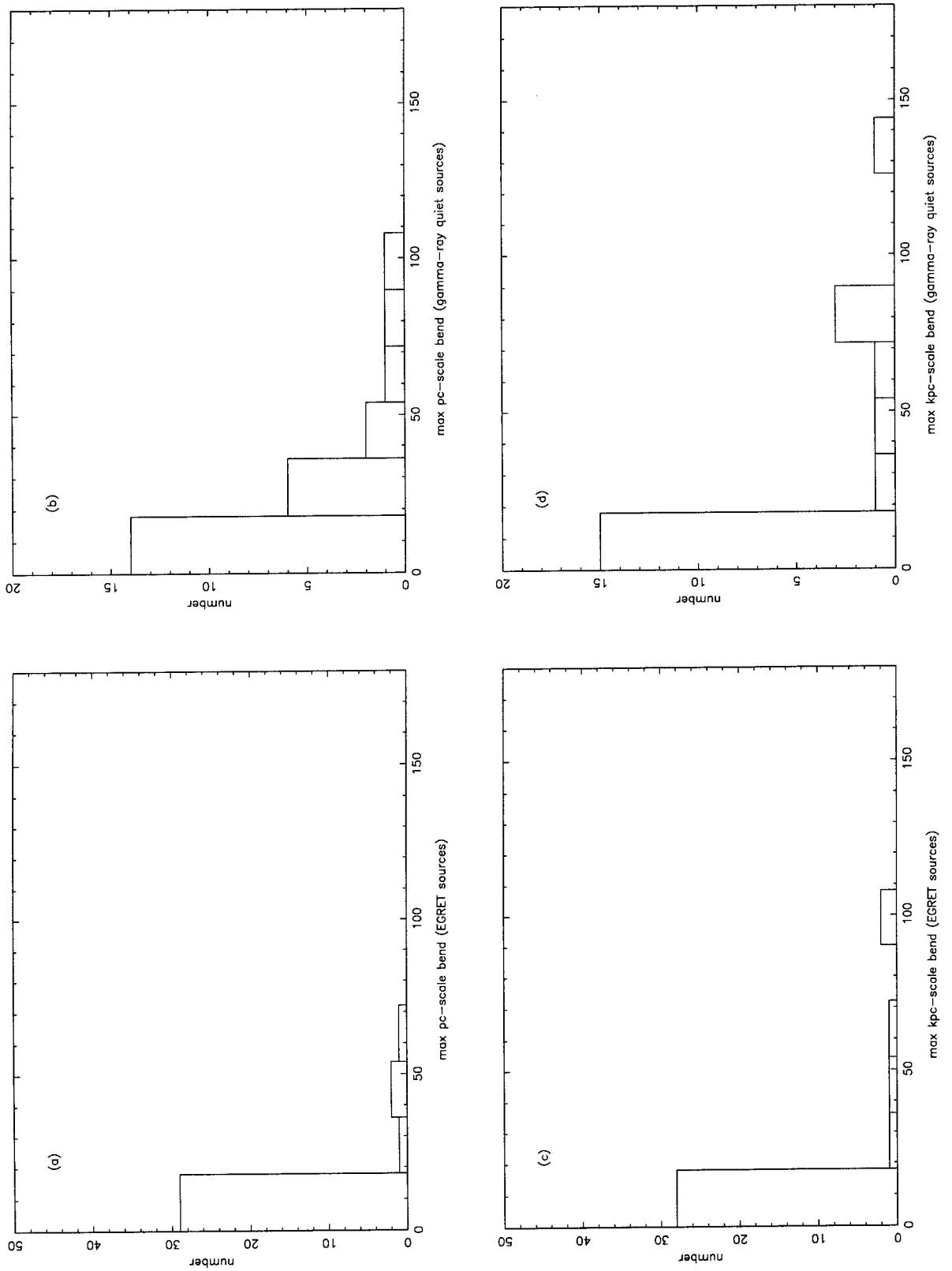
(a)
number
max pc–scale bend (EGRET sources)
(b)
number
max pc–scale bend (gamma–ray quiet sources)
(c)
number
max kpc–scale bend (EGRET sources)
(d)
number
max kpc–scale bend (gamma–ray quiet sources)

Fig. 10.—

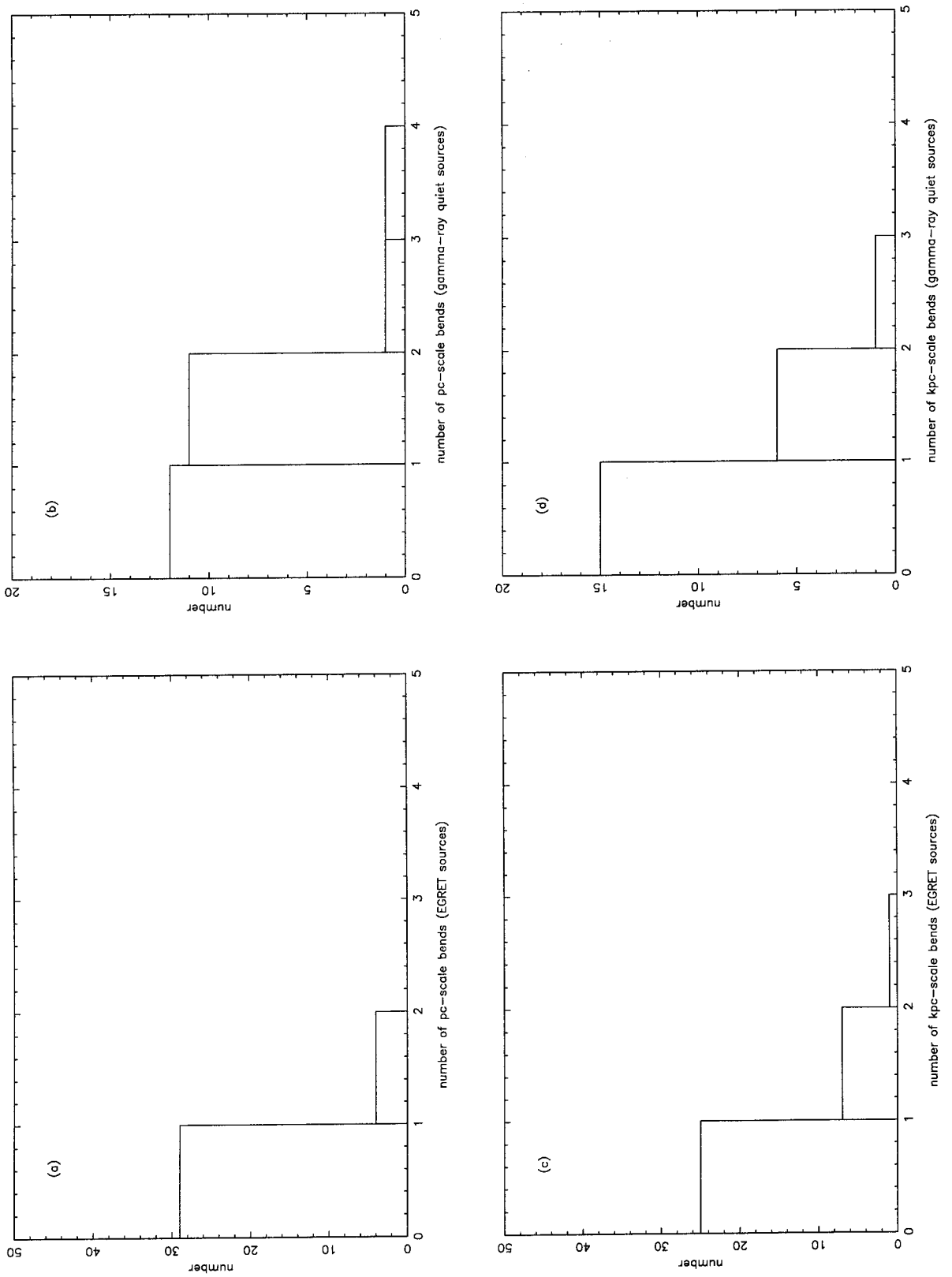
(a)
number
number of pc–scale bends (EGRET sources)
(b)
number
number of pc–scale bends (gamma–ray quiet sources)
(c)
number
number of kpc–scale bends (EGRET sources)
(d)
number
number of kpc–scale bends (gamma–ray quiet sources)

Fig. 11.—

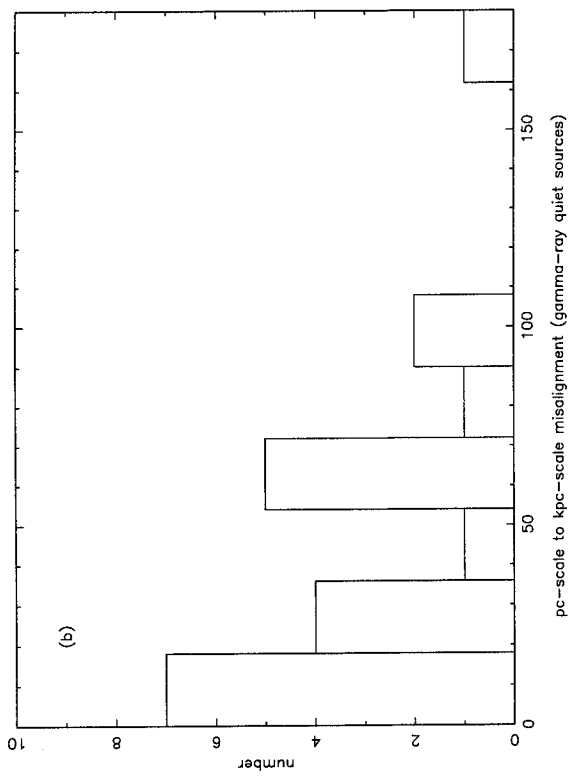
(b)
number
0
2
4
6
8
10
0
50
100
150
pc–scale to kpc–scale misalignment (gamma–ray quiet sources)

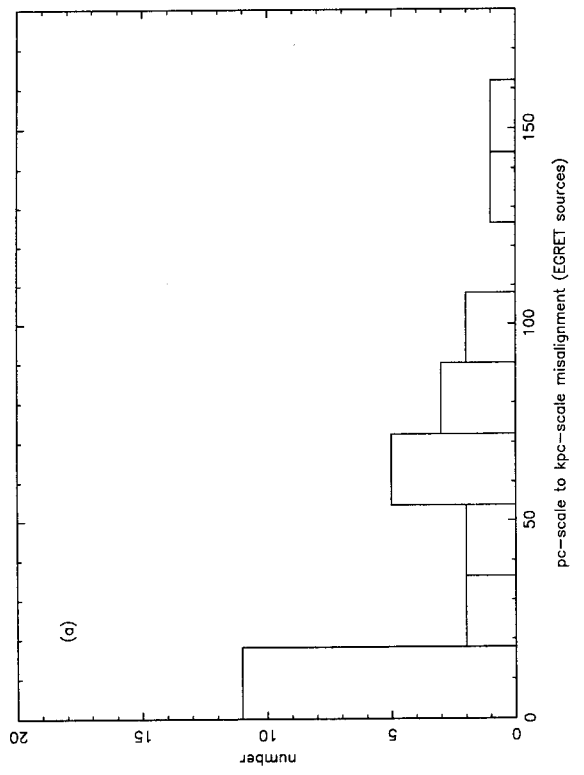
(a)
number
0
5
10
15
20
0
50
100
150
pc–scale to kpc–scale misalignment (EGRET sources)

Fig. 12.—